# Macromolecules

Volume 26, Number 13 June 21, 1993



## Plasma Deposition of Ultrathin Films of Poly(2-hydroxyethyl methacrylate): Surface Analysis and Protein Adsorption Measurements

**Gabriel P. López,† Buddy D. Ratner,* Richard J. Rapoza,‡ and Thomas A. Horbett**

*Center for Bioengineering and Department of Chemical Engineering, BF-10, University of Washington, Seattle, Washington 98195*

*Received October 9, 1991; Revised Manuscript Received January 26, 1993*

ABSTRACT: A method for the preparation of ultrathin films of poly(2-hydroxyethyl methacrylate) (PHEMA) by simultaneous condensation and RF plasma deposition of 2-hydroxyethyl methacrylate (HEMA) is described. Interactions of proteins with plasma-deposited and model PHEMA surfaces (spin-cast PHEMA, radiation-grafted PHEMA, and bulk PHEMA gels) were examined. Films prepared by conventional plasma deposition (i.e., without enhancing HEMA condensation by substrate temperature reduction) were also studied. $^{125}$I-radiolabeled fibrinogen was used to study the protein adsorption and retention characteristics of these materials. Kinetic protein adsorption and free iodide uptake studies were performed. In addition, gravimetric analysis, X-ray photoelectron spectroscopy, static secondary ion mass spectrometry, and water contact angle measurements were made to compare physical and chemical properties of the various hydrogel specimens and to gain insight into the reasons for their different protein interactions. Results demonstrate that plasma deposition of HEMA on substrates at low substrate temperatures is a viable method for preparing ultrathin, hydrogel films for biomedical applications.

### Introduction

Interest in the late 1970s in hydrogels for biomedical applications, especially for contact lens and blood-compatible surfaces, stimulated detailed investigation of the bulk and surface properties of poly(2-hydroxyethyl methacrylate) (PHEMA) gels.[1-4] Since that time, investigations of PHEMA for application in a myriad of biomedical devices has continued. PHEMA's chemical stability, swelling, and permeation characteristics have made this polymer, and various copolymers of 2-hydroxyethyl methacrylate (HEMA), desirable in applications such as drug release systems,[5-8] membrane dialyzers,[9] wound dressings,[10,11] testicular prostheses,[12] cell separation systems,[13-16] enzyme immobilizations,[17] intraocular lenses,[18,19] implant electrodes,[20] bone tissue substitutes,[21] cell microencapsulation,[22-24] and vocal cord prostheses.[25] Several fundamental studies on protein interactions with PHEMA and its copolymers have also been published.[26-28]

Radiation grafting of PHEMA has been used to treat devices such as vascular prostheses where a surface with a hydrophilic, gel-like character is desired on a substrate with specific mechanical properties.[10,29-32] The disadvantages of radiation grafting include (1) difficulty in control of graft thickness, (2) radiation damage to the substrate, (3) graft surface roughness, and (4) interpenetration of graft polymer into the substrate.

Radio frequency (RF) plasma deposition of PHEMA films should overcome many of these disadvantages and offers other advantages inherent in the plasma deposition technique. For example, the energetic plasma particle interactions with the substrate are limited to the surface region of the solid. Hence, substrates may be coated without change in their bulk mechanical properties.[33] Other advantages include film uniformity and the ability to coat many types of substrates of different geometry and chemistry.[33]

Films deposited from glow discharge plasmas produced using HEMA vapor have previously been studied in our laboratory for biomaterial applications, but chemical analysis and biological assays have shown that resultant films differ from solution polymerized PHEMA.[34,35] The origin of these differences stems from the high degree of fragmentation of HEMA that can occur during the plasma deposition process.[36] The interaction of neutral, gas-phase HEMA molecules with energetic plasma species such as

* Author to whom correspondence should be addressed.
† Current address: Department of Chemistry, Harvard University, Cambridge, MA 02138.
‡ Current address: Peripheral Systems Group Inc., 1395 Charleston Rd., Mountain View, CA 94043.

0024-9297/93/2226-3247$04.00/0 

electrons, ions, and electromagnetic radiation results in fragmentation of HEMA to form chemically reactive species that participate in reactions leading to film growth. The incorporation of these stochastically fragmented species, together with the molecular disruption that can occur on the surface of the film by energetic particle bombardment, results in the highly cross-linked and complex chemistry observed in the plasma-deposited films.[37]

Our goal has been to understand the processes that lead to these complex film chemistries and to develop new methodologies to control the chemical properties of plasma-deposited films. We have succeeded toward this end by developing the process of simultaneous condensation and plasma deposition for the control of precursor fragmentation.[37]

In this paper, we describe the RF plasma deposition of HEMA at reduced substrate temperatures to obtain ultrathin films that retain PHEMA-like qualities and are therefore useful for biomedical applications. Because of the role of protein adsorption in blood coagulation and in receptor-mediated cell adhesion phenomena in general, the biological interactions of films were appraised by comparing their protein (fibrinogen) adsorption and retention with that of several types of PHEMA prepared by conventional methods. These include solvent-soluble PHEMA spin-cast onto glass; chemically-initiated, bulk PHEMA cross-linked gels; and PHEMA radiation-grafted onto polyethylene. In addition, comparison to HEMA plasma-deposited films prepared without substrate cooling is made.

Because of the complex nature of these materials, a multitechnique analysis of the various films and gels is also presented. This includes comparisons of wettability and surface chemistry for the various types of gels. Chemical analyses include X-ray photoelectron spectroscopy (XPS) and static secondary ion mass spectrometry (SIMS). Correlation of film properties with protein interactions is also made.

## Experimental Section

**Materials.** The components of the capacitively coupled, external electrode, RF plasma reactor used for deposition have been described elsewhere.[38] Modifications of the tubular, glass deposition chamber to allow cooling of substrates with liquid nitrogen during the plasma deposition have also been described.[37] HEMA was heated to increase its vapor pressure, and its flow into the reactor was regulated by a Teflon stopcock. Pressure of the plasma during deposition was maintained at 0.2 Torr, and 20-W RF power was supplied. Polyethylene, pressed between mirror-finished aluminum plates, was used as the substrate material. Samples were etched in an argon plasma (40 W, 0.175 Torr, 5 min) immediately before deposition. Samples cooled with liquid nitrogen during deposition were treated for 5 min. Deposition time for samples coated without cooling was 15 min. Ophthalmic-grade HEMA (Polysciences, Inc., Warrington, PA) was used in all syntheses and depositions.

Chemically-initiated PHEMA gels were prepared with 3.3 mol % tetra(ethylene glycol) dimethacrylate (Scientific Polymer Products, Inc.) as a cross-linking agent in a solvent system of ethylene glycol/water. The exact gel formulation and conditions of polymerization can be found elsewhere.[39] HEMA was radiation-grafted by placing pressed polyethylene in 12% HEMA in ethanol/water (90.6/9.4 v/v) and irradiating for 18 h (0.25 Mrads) in a $^{60}Co$ source. Soluble poly(HEMA) (radiation-initiated) was cast from solution onto glass disks that had been previously coated with an ethyl methacrylate (Aldrich Chemical Co.)/(γ-methacryloxypropyl)trimethoxysilane (PCR Research Chemicals, Inc.) copolymer (2.5% EMA–silane in ethyl acetate) as a coupling agent. PHEMA (5%) in dimethyl formamide solution was spin-cast at 4500 rpm for 20 s on the EMA–silane treated glass.

**Fibrinogen Adsorption.** Fibrinogen was isolated from baboon blood, labeled with $^{125}I$, and characterized as described previously.[40] Protein adsorption was performed in a citrate phosphate-buffered saline buffer (pH 7.4) containing 0.02% sodium azide as a preservative and 0.01 M NaI to prevent nonspecific uptake of free $^{125}I$ during protein adsorption. Details of the adsorption and elution procedure are given elsewhere.[41] Briefly, adsorptions were initiated by adding 1 volume of protein stock solution to 2 volumes of buffer that contained a completely submerged test specimen at 37 °C. They were terminated by displacing the protein solution with buffer. The radioactivity on these samples yielded the initial protein adsorption. Elution was carried out by immediately submerging the test samples in a 3% sodium dodecyl sulfate (SDS) solution following adsorption. After rinsing the samples again, the retained radioactivity yielded the amount of protein remaining on the samples after elution. Samples were examined for preferential uptake of unbound $^{125}I$ by soaking in buffer solution of $^{125}I$ radioactivity equivalent to 1% of that in the protein solution used for adsorption experiments.

**Physical Characterization.** Wet and dry weights of the various types of PHEMA samples were measured using a Cahn Model G electrobalance (Cahn Instrument Co., Paramount, CA). Wet samples were blotted with filter paper prior to weighing. Electron micrographs were obtained using a JEOL JSM-25 scanning electron microscope (JEOL Ltd., Tokyo, Japan).

**Chemical Analysis.** X-ray photoelectron spectroscopy (XPS) analyses were done on an SSX-100 surface analysis system (Surface Science Instruments, Mountain View, CA) using a monochromatic Al Kα X-ray source and a detection system with a 30° solid angle acceptance lens, a hemispherical analyzer, and a position-sensitive detector. Survey scans (0–1000-eV binding energy) were run at an analyzer pass energy of 150 eV and an X-ray spot size of 1000 μm to determine the elemental composition of each film sample. High-resolution $O_{1s}$ and $C_{1s}$ spectra were obtained at a pass energy of 25 eV and varying spot sizes. A low-energy electron flood gun set at 5 eV was used to minimize sample charging. The high-resolution spectra were resolved into individual Gaussian peaks using a least squares fitting program. All binding energies (BE's) were referenced by setting the maximum of the resolved $C_{1s}$ peak corresponding to carbon in a hydrocarbon environment ($CH_x$) to 285.0 eV.

SIMS analyses of the various sample surfaces were also done on the SSX-100 surface analysis system. The primary ion source was a 3.5-keV, 1.5-nA $Xe^+$ beam produced from a differentially pumped Leybold-Heraeus ion gun. The sample was bombarded over a 3-mm-diameter area during data acquisition. The total ion dose during data acquisition was $<1 \times 10^{13}$ ions/cm$^2$, which ensured that static SIMS conditions were met.[42] The secondary ions were detected by a modified QMG 511 Balzers quadrupole mass spectrometer equipped with an adjustable energy filter. The takeoff angle of the detected secondary ions was near normal. A low-energy electron flood gun set at 32 eV (positive secondary ions) or 80 eV (negative secondary ions) was used to minimize sample charging.

## Results

**Protein Interaction Measurements.** The amount of fibrinogen adsorbed to the various PHEMA samples exposed to 0.1 mg/mL protein solution for 1 min, 10 min, and 2 h is shown in Figure 1. HEMA plasma-deposited at low temperature (HEMA-PDLT) adsorbs approximately the same amount of fibrinogen as the radiation-grafted PHEMA and the PHEMA gel over the adsorption times measured. HEMA deposited without substrate cooling (HEMA-PDHT), however, adsorbs much higher levels of fibrinogen, especially at the longer adsorption times. Another interesting feature of this plot is that the spin-cast PHEMA samples adsorb less protein than the other samples at longer adsorption times. Furthermore, the amount of adsorbed protein does not vary significantly with adsorption time for the spin-cast samples. These differences in adsorption amount and kinetics are likely

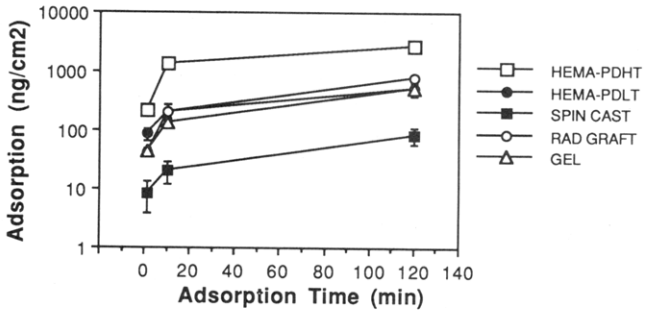


**Figure 1.** Amount of fibrinogen adsorbed from a 0.1 mg/mL solution in buffer (37 °C) to PHEMA specimens prepared by various methods. Each data point represents a mean ($n$ = 3) ± SD.

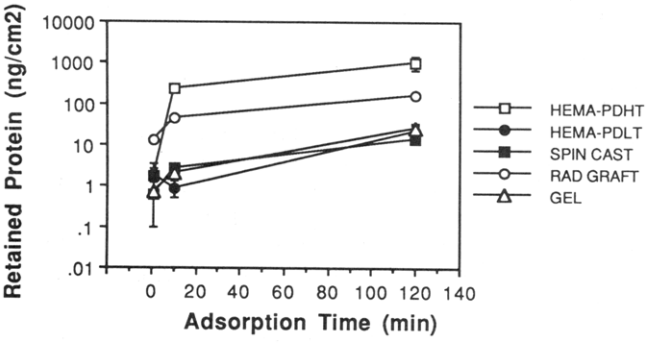


**Figure 2.** Amount of fibrinogen retained on various PHEMA specimens after 24-h SDS elution at 37 °C.

to be indicative of differences in surface chemistry, mobility, or morphology in the various types of samples.

The amount of fibrinogen retained after 24-h elution with SDS surfactant for the various adsorption times is shown in Figure 2. Again, HEMA-PDLT exhibited behavior similar to the PHEMA gel in that the amount of retained protein is similar for all adsorption times. The spin-cast PHEMA samples retained comparable amounts of fibrinogen over the adsorption times studied as well. Comparison at these low protein levels (<10 ng/cm$^2$) is suspect, however, because the measured radioactivity was near background. In contrast to the protein adsorption, the elutability of the radiation-grafted PHEMA was not similar to that of the other PHEMA samples in that the fraction of retained protein was higher for all adsorption times. In addition, the HEMA-PDHT samples exhibited elutability different from that of all other samples after 10-min and 2-h fibrinogen adsorptions.

The possibility of artifacts in the protein adsorption data was examined by considering that uptake of free $^{125}$I might occur during the adsorption experiments. Since there were large differences in the total mass of PHEMA in the various types of samples, the potential to retain widely differing amounts of $^{125}$I in the bulk hydrogel was a concern. Even though Na$^{123}$I was added to the buffer solution and the protein solution was dialyzed and tested for free $^{125}$I before adsorption, investigation of $^{125}$I binding to artifactually skew the results was essential. Figure 3 shows the free iodide uptake for the various samples. As expected, those samples with a greater amount of hydrogel absorbed more iodide. The PHEMA gel and the radiation graft (which was the thickest graft, 2.0 mg/cm$^2$) retained the highest amounts of $^{125}$I. By comparison, spin-cast PHEMA and HEMA-PDLT (0.054 mg/cm$^2$) retained very low levels of iodide. HEMA-PDHT retained approximately the same level of $^{125}$I as the radiation graft, even though the average graft weight (0.016 mg/cm$^2$) was less than that of HEMA-PDLT.

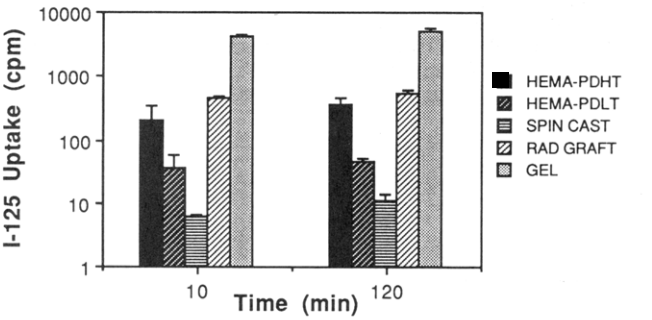


**Figure 3.** Amount of free $^{125}$I uptake by PHEMA prepared by the various methods.

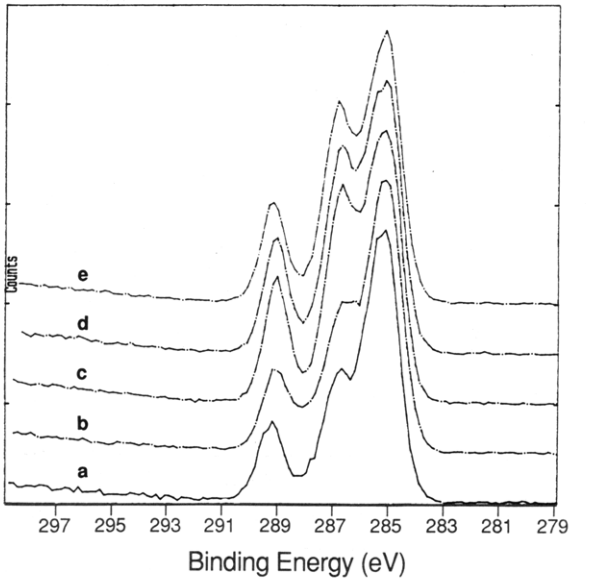


**Figure 4.** XPS $C_{1s}$ spectra of the PHEMA samples prepared by the various methods: (a) HEMA-HT, (b) HEMA-LT, (c) spin-cast PHEMA, (d) radiation-grafted PHEMA, and (e) PHEMA gel.

**Chemical Analysis.** Table I summarizes the XPS data for the various types of surfaces. Elemental compositions, reported here as carbon-to-oxygen ratios (C/O), were obtained by comparing intensities of core-level photoelectron emission for different elements. Within the typical error of the XPS measurement, the spin-cast, radiation-grafted, and cross-linked gel PHEMA samples showed C/O's approximately equal to that expected from the theoretical PHEMA composition (C/O = 2.0). C/O ratios were consistently higher than 2.0 (~2.3), however. This may be due to low levels of hydrocarbon contamination on the polymer surfaces. The PHEMA gel contained another contaminant that was detected as a silicon signal in the XPS spectrum (~3 atom % Si). We have had difficulties removing this contaminant from the gels, and the extent to which it may influence measurement of protein interactions or wettability is not certain. None of the other plasma-deposited samples or PHEMA samples showed peaks from elements other than carbon and oxygen in their XPS spectra. The plasma-deposited surfaces also showed C/O's higher than the theoretical C/O for PHEMA, but approximately the same as those for the PHEMA samples.

High-resolution $C_{1s}$ and $O_{1s}$ core-level spectra were also examined. These spectra reflect the types of carbon and oxygen functional groups present in the various surfaces. Figure 4 shows representative $C_{1s}$ spectra for the five types of surfaces. The spectra were resolved into three peaks: (1) a 285.0-eV peak corresponding to carbon with no bonds

**Table I. XPS Carbon-to-Oxygen Elemental Percentage Ratios (C/O) and Resolved High-Resolution $C_{1s}$ Area Ratios for the Various PHEMA Specimens (Based on a Three-Peak Fit to the Spectra)**

| | | $C_{1s}$ peak area ratios | | |
|---|---|---|---|---|
| specimen | C/O | 288.9 eV | 286.6 eV | 285.0 eV |
| HEMA-PDHT | 2.6 | 1 | 2.2 | 4.1 |
| HEMA-PDLT | 2.5 | 1 | 2.1 | 3.3 |
| spin-cast PHEMA | 2.3 | 1 | 2.3 | 2.9 |
| radiation-grafted PHEMA | 2.4 | 1 | 2.4 | 3.0 |
| PHEMA gel | 2.3 | 1 | 2.5 | 3.4 |
| theory | 2.0 | 1 | 2 | 3 |

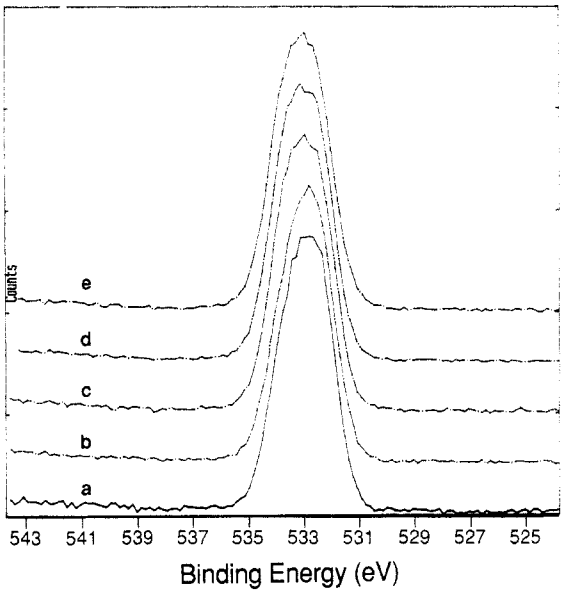


**Figure 5.** XPS $O_{1s}$ spectra of the PHEMA samples prepared by the various methods: (a) HEMA-HT, (b) HEMA-LT, (c) spin-cast PHEMA, (d) radiation-grafted PHEMA, and (e) PHEMA gel.

to oxygen ($CH_x$, hydrocarbons), (2) a 286.6-eV peak corresponding to carbon with one oxygen bond (*C*—O, ethers and alcohols), and (3) a 288.9-eV peak corresponding to carbons with three bonds to oxygen (O=*C*—O, esters). The spectra in Figure 4 can alternatively be fit with an additional peak due to a secondary chemical shift induced by the ester group on the substituted backbone carbon.[43,44] For the purposes of comparison, though, the simpler three-peak fit was used.

The ratios of the resolved peaks are tabulated in Table I. As expected from the polymer structure, the areas of the three component peaks, for the PHEMA samples, are approximately in the ratio of 3:2:1 ($CH_x$:*C*—O:O=*C*—O). Although differences in the line shape of the spectra are apparent, especially between the plasma-deposited samples and the PHEMA samples (prepared without plasma deposition), the resolved peak area ratios indicate similar amounts of each type of carbon for all the films. The plasma-deposited films showed similar spectra, although the peak resolution indicated HEMA-PDHT had slightly higher levels of hydrocarbon-type carbons. In addition, in the plasma-deposited films, the shoulder indicative of *C*—O is less well-resolved from the $CH_x$ peak than PHEMA specimens fabricated without plasma deposition.

Figure 5 compares representative high-resolution $O_{1s}$ spectra for the various specimens. Although only one symmetric peak is present in the PHEMA spectra (spin-cast, gel, radiation graft), model compound studies have shown distinct binding energies for the three types of oxygens in the PHEMA repeat unit.[45] The hydroxyl oxygen (H—*O*—C ~532.8 eV), the carbonyl oxygen in the ester (*O*=C—O ~532.2 eV), and the ester linkage oxygen (O=C—*O*—C ~533.7 eV) are present in the HEMA repeat unit in the ratio 1:1:1 and yield a symmetric $O_{1s}$ envelope.[45] The plasma-deposited films yielded $O_{1s}$ spectra that were slightly asymmetric, with a depletion of high binding energy components suggesting a reduction in ester-linked oxygens (O=C—*O*—C).

Figure 6 shows the positive ion SIMS spectra of the spin-cast PHEMA, the radiation-grafted PHEMA, and the plasma-deposited HEMA films. Comparison of the positive ion spectra for the radiation-grafted PHEMA and the spin-cast film shows that materials prepared by these two methods produce similar fingerprint spectra. These spectra agree well with previously published positive ion PHEMA spectra in both the mass and the relative intensity of the ions detected.[46,47] One notable exception is the conspicuous $m/z$ = 149 peak in these spectra, which is not present (or present at very low intensity) in the previously published spectra. The ion fragment (or fragments) responsible for this peak may be attributable to a contaminant on the specimen surfaces. An $m/z$ = 149 peak has been observed when other plasma-deposited films synthesized in our laboratory have been analyzed. Such a peak may be due to phthalate cation ($C_8H_5O_3^+$). Studies to verify this peak assignment using derivatization SIMS and high mass resolution SIMS are planned.

Comparison of the positive ion spectra of the plasma-deposited films shows that peak clusters similar to those of non-plasma-deposited PHEMA specimens are observed, especially below $m/z$ = 100. Differences in peak intensities between the PHEMA films produced with and without plasma deposition are obvious, but HEMA-PDHT and HEMA-PDLT generally look similar in this region. Above $m/z$ = 100, a conspicuous difference between the two plasma-deposited samples is observed. The characteristic $m/z$ = 113 peak (which is prominent in all the non-plasma-deposited PHEMA samples) is much more intense in the HEMA-PDLT spectrum than in the HEMA-PDHT spectrum. This peak has been assigned to an ion fragment consisting of the PHEMA repeat unit without the side chain terminal hydroxyl group ($C_5H_9O_2^+$).[46] We believe that the intensity of this peak is an indication of HEMA fragmentation occurring during the plasma deposition procedure. The ratio of this peak to other dominant positive ion peaks (e.g., $m/z$ = 43) for HEMA-PDLT is much closer to that observed in the spin-cast and radiation-grafted PHEMA than for HEMA-PDHT. This suggests that HEMA suffers less fragmentation when it is used in plasma deposition on cooled substrates.

Figure 7 shows the negative ion SIMS spectra for the plasma-deposited and non-plasma-deposited PHEMA specimens. Again, the fingerprint spectra for the radiation-grafted and the spin-cast film are similar and agree well with published PHEMA spectra. Substantial differences are seen in the total intensity of molecular ion peaks for these samples that may be related to the degree of cross-linking in the polymer network. We have investigated the effects of cross-link density on ion yield in SIMS and have found reduced total ion yield for polymers with higher cross-link densities.[48] In negative ion SIMS, the HEMA-PDLT spectrum is similar to the PHEMA spectra, indicating similar chemical structures in these films. The negative ion spectra of the HEMA-PDHT films were dramatically different from the PHEMA spectra, however, with a loss of most molecular information above $m/z$ = 25. This indicates that these films are of substantially different nature than the other films analyzed and are consistent

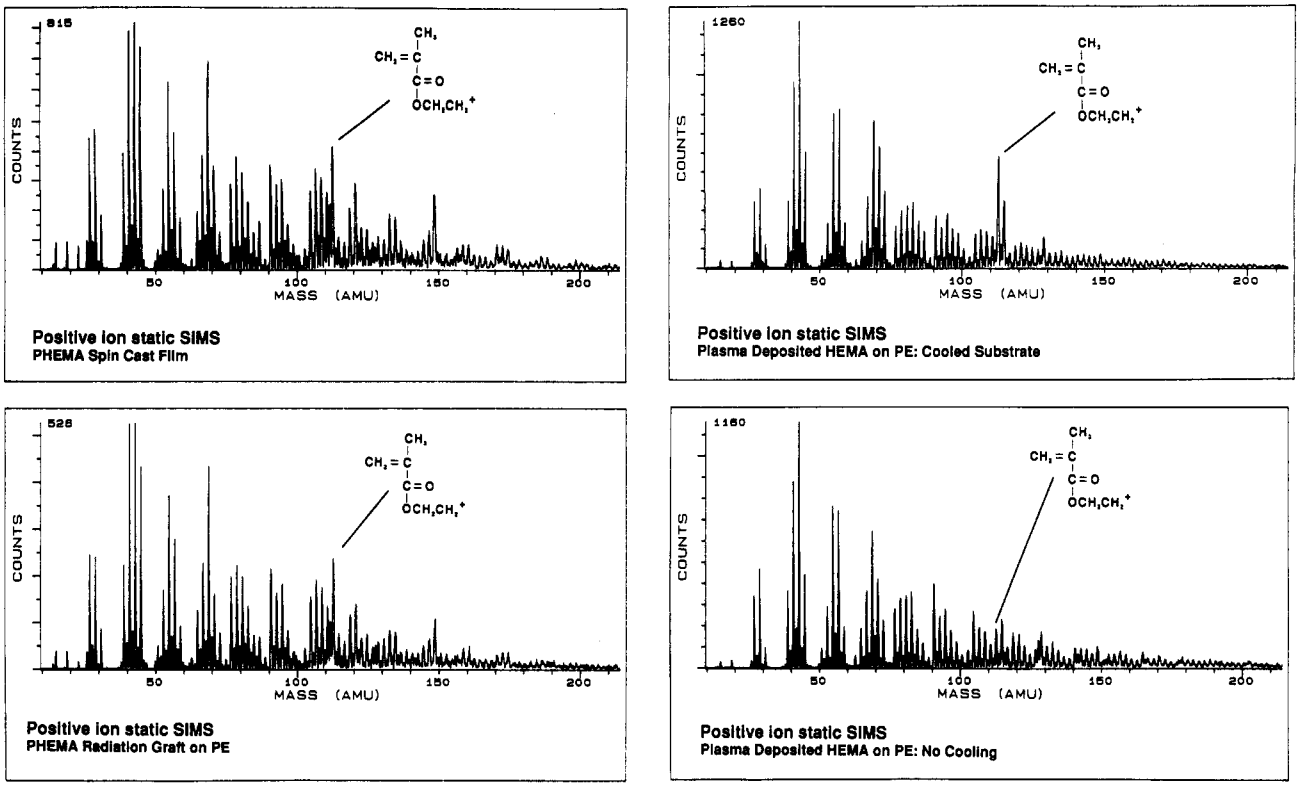


**Figure 6.** Positive ion static SIMS spectra of PHEMA samples prepared by the various methods.

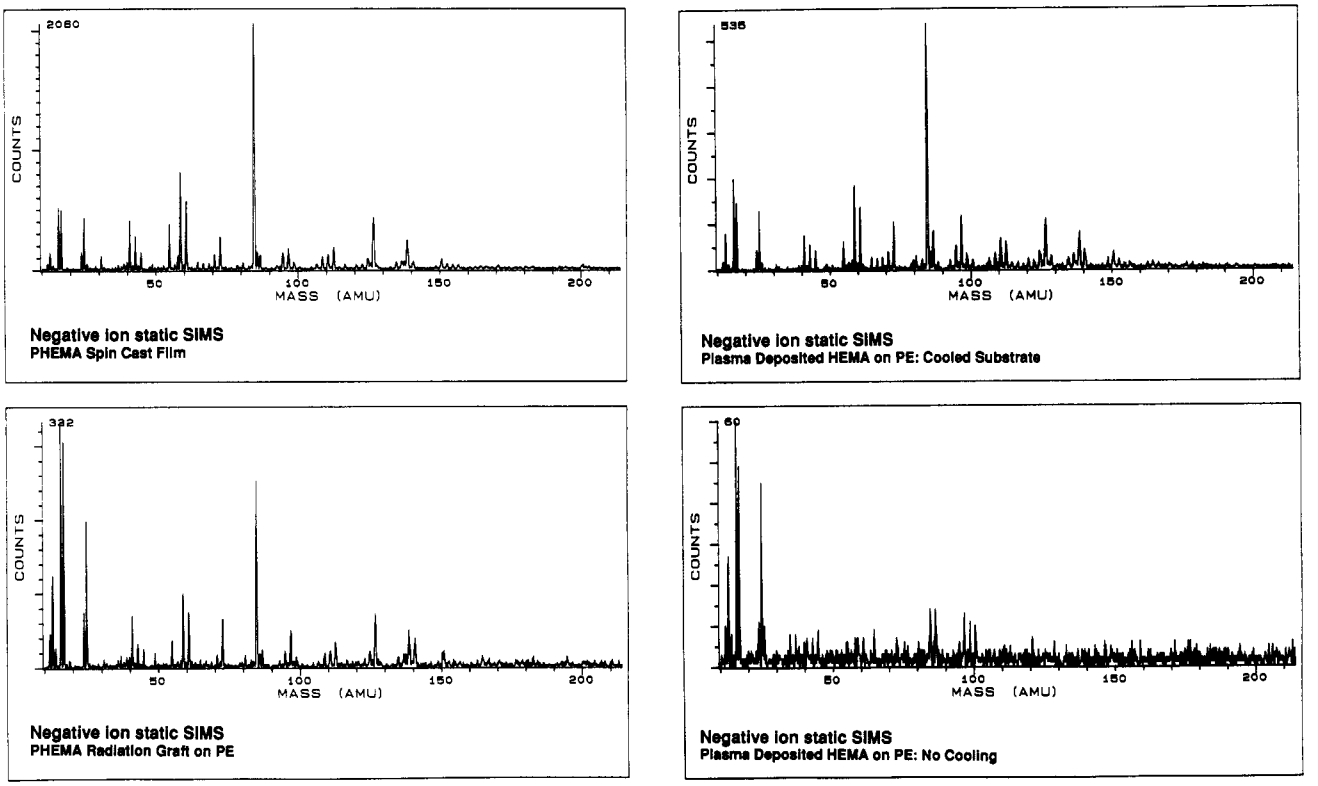


**Figure 7.** Negative ion static SIMS spectra of PHEMA samples prepared by the various methods.

with highly cross-linked HEMA polymers examined in the study cited above.

## Discussion

The relative abundance of fibrinogen in blood, its high surface activity, and its key role in coagulation makes this protein a central player in early adsorption events after blood–material contact. The role of fibrinogen in later events such as platelet adhesion and spreading has also been explored.[35,49,50] Both protein adsorption and protein retention after elution with surfactant have been shown to depend on a variety of chemical and morphological properties of polymers.[41]

Fibrinogen adsorption measured for the HEMA-PDHT samples was high (~2800 ng/cm$^2$ after 2 h of adsorption) compared to the other PHEMA types studied. Comparable levels have been measured for fibrinogen adsorption to other polymers.[51] These levels are in the range of adsorption expected for end-on fibrinogen monolayer

coverage (2200–4000 ng/cm$^2$).[50] We, at present, however, cannot rule out multilayer adsorption.

Even though the graft level for the HEMA-PDHT samples was low and similar to that for the HEMA-PDLT samples, they retained significantly more iodide than the HEMA-PDLT samples. This may be due to specific iodide adsorption or interaction of iodide with chemical groups (not found in PHEMA) produced during the deposition process. The amount of protein adsorption corresponding to this $^{125}$I retention is small, however (less than 30 ng/cm$^2$ for both 10-min and 2-h adsorptions), compared to the actual protein adsorption measured at both adsorption times (see Figure 1). The independence of iodide uptake with adsorption time suggests that uptake was near saturation. These results lend credibility to the protein interaction measurements in that they indicate that artifacts associated with the retention of $^{125}$I during the protein adsorption measurements were minimal.

XPS gives quantitative information on the elemental composition and molecular environment of approximately the top 100 Å of a surface and is therefore ideally suited for analyzing thin films.[52,53] Static SIMS is an excellent complement to surface analysis by XPS because it is rich in information on the chemical structure in the uppermost 10–15 Å of a polymer surface.[54,55] Hearn and Briggs have studied both the positive and negative SIMS spectra of spin-cast PHEMA and have assigned ion structures to the major peaks.[46] Brown and Vickerman have also independently published PHEMA SIMS spectra and discussed peak assignments.[47] These published results provide fingerprint spectra to which we can compare SIMS spectra of PHEMA specimens.

We have presented here a brief analysis that compares SIMS spectral fingerprints to demonstrate the similarity of the SIMS spectra of the various PHEMA's to previously published PHEMA spectra. A more complete analysis of the spectra of the plasma-deposited HEMA (both HEMA-PDLT and HEMA-PDHT) and a more detailed interpretation of the consequences of plasma deposition on monomer scrambling is published elsewhere.[56]

Briefly, both the positive and negative ion spectra indicate that the surface chemistry of the spin-cast and gel PHEMA surfaces are similar, and are similar to the chemistry of the HEMA-PDLT surface, as well. However, the SIMS spectra (positive and negative) indicate that the surface chemistry of the HEMA-PDHT samples is substantially different. Both positive and negative ion SIMS spectra provide evidence that the degree of HEMA fragmentation occurring during plasma deposition is lower when low substrate temperatures are used.

Additional evidence for the increased fragmentation of HEMA-PDHT was obtained from underwater, air contact angle measurements. The spin-cast PHEMA showed a substantially higher contact angle, indicating lower wettability, while the HEMA-PDHT sample showed the highest wettability. This may be due to hydroxyl groups in the HEMA-PDHT sample trapped, because of cross-linking, in a conformation where they must point outward to the interface. Unlike the spin-cast PHEMA, HEMA-PDHT has no conformational possibility to rearrange. This wettability phenomenon for these plasma-deposited films will be described in more detail elsewhere.[57] Others have discussed aspects of mobility and contact angles for plasma-deposited films[58–59] and hydrogel films.[60]

There are several chemical factors that may influence protein adsorption and that may be altered as a result of increased fragmentation of HEMA during plasma deposition. These may include surface energy, the degree of steric repulsion of proteins by hydrated polymer chains (which may be influenced by polymer mobility), and the presence of molecular-level heterogeneities in surface chemistry produced as a consequence of the production of new functional groups during the plasma deposition. Such new functional groups may give rise to specific interactions (e.g., ionic) between the protein and the plasma-deposited film.

## Conclusions

Fibrinogen interaction measurements suggest that the HEMA-PDLT films will interact with biological systems similarly to other PHEMA grafts. There may be several advantages of the plasma deposition process over other film grafting procedures (e.g., radiation grafting) including ready control of film thickness and the ability to make ultrathin films. Thus, the simultaneous condensation–plasma deposition of HEMA may be a desirable surface treatment for many types of biomaterials applications.

Chemical analyses and contact angle measurements also showed that the HEMA-PDLT films were similar in nature to conventional PHEMA grafts and gels. Although XPS analysis was relatively insensitive to differences in surface chemistry, especially between the HEMA-PDLT and HEMA-PDHT films, static SIMS analysis showed clear differences. However, XPS did provide useful surface elemental composition information that cannot be obtained by other means.

These experiments also explore the value of protein interaction studies as a comparative probe for the surface structure of polymers. The difference in fibrinogen uptake and retention between the spin-cast samples and the other PHEMA samples (radiation grafts) may explain earlier observations on differences in platelet consumption of PHEMA surfaces prepared by different methods.[61] Because of the sensitivity of protein–polymer interactions to surface chemistry and macromolecular structure, protein interaction measurements may be useful in the general comparison of difficult-to-characterize polymer surfaces.

All analyses performed indicated that by plasma-depositing HEMA at low temperature, a polymeric graft similar in nature to conventional PHEMA can be prepared. HEMA serves as a model system for other useful methacrylate- and acrylate-based thin film systems that may find application in the fields of biomaterial and material technology.

**Acknowledgment.** We are grateful for technical assistance provided by Winston Ciridon, David G. Castner, and Deborah Leach-Scampavia (University of Washington) and support for this research provided by the Washington Technology Center and the NIH through Grant RR01296. We also thank Thomas M. Menduni for his assistance in editing this manuscript.

## References and Notes

(1) Ratner, B. D.; Hoffman, A. S. In *Hydrogels for Medical and Related Applications*; Andrade, J. D., Ed.; ACS Symposium Series; American Chemical Society: Washington, DC, 1976.
(2) Ratner, B. D. In *Biocompatibility of Clinical Implant Materials*; Williams, D. F., Ed.; CRC Press: Boca Raton, FL, 1981.
(3) Peppas, N. A.; Yang, W. H. M. *Contact Intraocul. Lens Med. J.* **1981**, *7*, 300.
(4) Hoffman, A. S.; Cohn, D. C.; Hanson, S. R.; Harker, L. A.; Horbett, T. A.; Ratner, B. D.; Reynolds, L. O. *Radiat. Phys. Chem.* **1983**, *22*, 267.
(5) Sefton, M. V.; Nishimura, E. *J. Pharm. Sci.* **1980**, *69*, 208.
(6) Denizli, A.; Kiremitci, M.; Piskin, E. *Biomaterials* **1988**, *9*, 363.
(7) Robert, C. C. R.; Buri, P. A.; Peppas, N. A. *J. Controlled Release* **1987**, *5*, 151.

(8) Albin, G.; Horbett, T. A.; Ratner, B. D. *J. Controlled Release* **1985**, *2*, 153.
(9) Yuee, F.; Tianyi, S. *J. Membr. Sci.* **1988**, *39*, 1.
(10) Gourlay, S. J.; Rice, R. M.; Hegyeli, A. F.; Eaton, J. C.; Hodge, J. W.; Wade, C. W. R. *Trans.—Am. Soc. Artif. Intern. Organs* **1975**, *21*, 28.
(11) Meaburn, G. M.; Hosszu, J. L.; Coles, C. M. *Int. J. Appl. Radiat. Isot.* **1978**, *29*, 233.
(12) Yoshida, M.; Asano, M.; Kaetsu, I.; Imai, K.; Mashimo, T.; Yuasa, H.; Yamanaka, H.; Kawaharada, U.; Suzuki, K. *Biomaterials* **1987**, *8*, 124.
(13) Maruyama, A.; Tsuruta, T.; Kataoka, K.; Sakurai, Y. *Biomaterials* **1989**, *10*, 393.
(14) Kataoka, K. *Crit. Rev. Biocompat.* **1988**, *4*, 341.
(15) Kataoka, K.; Sakurai, Y.; Hanai, T.; Maruyama, A.; Tsuruta, T. *Biomaterials* **1988**, *9*, 218.
(16) Kataoka, K. *Artif. Organs* **1988**, *12*, 505.
(17) Arica, Y.; Hasirci, V. N. *Biomaterials* **1987**, *8*, 489.
(18) Chirila, T. V.; Russo, A. V.; Constable, I. J. *J. Cataract Refract. Surg.* **1989**, *15*, 504.
(19) Smetana, K., Jr.; Sulc, J.; Krcova, Z.; Pitrova, S. *J. Biomed. Mater. Res.* **1987**, *21*, 1247.
(20) Margules, G. S.; MacGregor, D. C.; Kane, J. A.; Livingston, A. R. *J. Biomed. Eng.* **1987**, *9*, 21.
(21) Korbelar, P.; Vacik, J.; Dylevsky, I. *J. Biomed. Mater. Res.* **1988**, *22*, 751.
(22) Stevenson, W. T. K.; Evangelista, R. A.; Sugamori, M. E.; Sefton, M. V. *Biomater., Artif. Cells, Artif. Organs* **1988**, *16*, 747.
(23) Stevenson, W. T. K.; Sefton, M. V. *Biomaterials* **1987**, *8*, 449.
(24) Dawson, R. M.; Broughton, R. L.; Stevenson, W. T. K.; Sefton, M. V. *Biomaterials* **1987**, *8*, 360.
(25) Kresa, Z.; Rems, J.; Wichterle, O. *Otolaryngology, Head Neck Surgery* **1988**, *98*, 242.
(26) Horbett, T. A. In *Adhesion and Adsorption of Polymers, Part B*; Lee, L. H., Ed.; Plenum Publishing: New York, 1980.
(27) Horbett, T. A. In *Biomaterials 1980, Advances in Biomaterials*; Winter, G. D., Ed.; John Wiley & Sons: Chichester, England, 1982.
(28) Horbett, T. A. In *Hydrogels in Medicine and Pharmacy*; Peppas, N. L., Ed.; CRC Press: Boca Raton, FL, 1986.
(29) Cohn, D.; Hoffman, A. S.; Ratner, B. D. *J. Appl. Polym. Sci.* **1984**, *29*, 2645.
(30) Fischer, J. P.; Becker, U.; Halasz, S. P.; Muck, K. F.; Puschner, H.; Rosinger, S.; Schmidt, A. In *Preprints for the 17th IUPAC Prague Microsymposium, Medical Polymers: Chemical Problems*; 1977.
(31) Hayashi, K.; Murata, K.; Yamamoto, N.; Yamashita, I. *Kobunshi Ronbunshu* **1985**, *42*, 77.
(32) Jansen, B. In *Biomaterials and Biomechanics 1983*; Ducheyne, P., Ed.; Elsevier Science Publishers: Amsterdam, 1984.
(33) Ratner, B. D.; Chilkoti, A.; Lopez, G. P. In *Plasma Deposition, Treatment and Etching of Polymers*; D'Agostino, R., Ed.; Academic Press: San Diego, 1990.
(34) Mateo, N. B.; Ratner, B. D. *Invest. Ophthalmol. Visual Sci.* **1989**, *30*, 853.
(35) Lopez, G. P.; Ratner, B. D. *J. Appl. Polym. Sci., Appl. Polym. Symp.* **1990**, *46*, 493.
(36) Winters, H. F.; Chang, R. P. H.; Mogab, C. J.; Evans, J.; Thornton, J. A.; Yasuda, H. *Mater. Sci. Eng.* **1985**, *70*, 53.
(37) For a more complete description of the mechanisms of this process and a review of the factors influencing molecular fragmentation during plasma deposition, see: Lopez, G. P.; Ratner, B. D. *Langmuir* **1991**, *7*, 766. Lopez, G. P.; Ratner, B. D. *J. Polym. Sci., Polym. Chem. Ed.* **1992**, *30*, 2415.
(38) Haque, Y.; Ratner, B. D. *J. Appl. Polym. Sci.* **1986**, *32*, 4369.
(39) Ratner, B. D.; Miller, I. F. *J. Polym. Sci., Polym. Chem. Ed.* **1972**, *10*, 2425.
(40) Bohnert, J. L.; Horbett, T. A. *J. Colloid Interface Sci.* **1986**, *111*, 363.
(41) Rapoza, R. J.; Horbett, T. A. *J. Colloid Interface Sci.* **1990**, *136*, 480.
(42) Hearn, M. J.; Briggs, D. *Surf. Interface Anal.* **1986**, *9*, 411.
(43) Pijpers, A. P.; Donners, W. A. B. *J. Polym. Sci., Polym. Chem. Ed.* **1985**, *23*, 453.
(44) Castner, D. G.; Ratner, B. D. *Surf. Interface Anal.* **1990**, *15*, 479.
(45) Lopez, G. P.; Castner, D. G.; Ratner, B. D. *Surf. Interface Anal.* **1991**, *17*, 267.
(46) Hearn, M. J.; Briggs, D. *Surf. Interface nal.* **1988**, *11*, 198.
(47) Brown, A.; Vickerman, J. C. *Surf. Interface Anal.* **1986**, *8*, 75.
(48) Chilkoti, A.; Lopez, G. P.; Ratner, B. D.; Hearn, M. J.; Briggs, D. *Macromolecules*, in press.
(49) Collins, W. E.; Mosher, D. F.; Diwan, A. R.; Murthy, K. D.; Simmons, S. R.; Albrecht, R. M.; Cooper, S. L. *Scanning Microsc.* **1987**, *1*, 1669.
(50) Ward, C. A.; Stanga, D. *J. Colloid Interface Sci.* **1986**, *114*, 323.
(51) Ward, C. A.; Stanga, D.; Zdasiuk, B. J.; Gates, F. L. *Ann. Biomed. Eng.* **1979**, *7*, 451.
(52) Dilks, A. In *Electron Spectroscopy: Theory, Techniques, and Applications*; Baker, A. D., Ed.; Academic Press: London, 1981.
(53) Ratner, B. D.; Castner, D. G. In *Surface Analysis—Techniques and Applications*, 1st ed.; Vickerman, J. C., Reed, N. M., Eds.; John Wiley & Sons: Chichester, U.K., in press.
(54) Castner, D. G.; Ratner, B. D. In *Surface Characterization of Biomaterials*; Ratner, B. D., Ed.; Elsevier: Amsterdam, 1988.
(55) Briggs, D. *Surf. Interface Anal.* **1986**, *9*, 391.
(56) Lopez, G. P.; Chilkoti, A.; Briggs, D.; Ratner, B. D. *J. Polym. Sci., Polym. Chem. Ed.* **1992**, *30*, 2427.
(57) Lopez, G. P.; Ratner, B. D., unpublished results.
(58) Yasuda, H.; Sharma, A. K.; Yasuda, T. G. *J. Polym. Sci., Polym. Phys. Ed.* **1981**, *19*, 1285.
(59) Yasuda, H. *Plasma Polymerization*; Academic Press: New York, 1985; pp 345–354.
(60) Holley, F. J.; Refojo, M. F. *J. Biomed. Mater. Res.* **1975**, *9*, 315.
(61) Hoffman, A. S.; Hanson, S. R.; Ratner, B. D.; Harker, L. A.; Reynolds, L. O. *Trans. Soc. Biomater.* **1982**, *5*, 36.